



# Characterization of the sequence distribution and crystalline structure of poly(ethylene-*co*-vinyl acetate) copolymers with high-resolution NMR spectroscopy

Zhiqiang Su<sup>a</sup>, Ying Zhao<sup>a</sup>, Yizhuang Xu<sup>b</sup>, Xiuqin Zhang<sup>a</sup>, Shannong Zhu<sup>a</sup>, Dujin Wang<sup>a,\*</sup>, Jinguang Wu<sup>b</sup>, Charles C. Han<sup>a</sup>, Duanfu Xu<sup>a,\*</sup>

<sup>a</sup>State Key Laboratory of Polymer Physics and Chemistry, Joint Laboratory of Polymer Science and Materials, Center for Molecular Science, Institute of Chemistry, Chinese Academy of Sciences, Zhongguancun, Beijing 100080, China

<sup>b</sup>State Key Laboratory of Rare Earth Materials Chemistry and Applications, College of Chemistry and Molecular Engineering, Peking University, Beijing 100871, China

Received 1 December 2003; received in revised form 18 March 2004; accepted 22 March 2004

## Abstract

The sequence distribution and crystalline structure of a series of poly(ethylene-*co*-vinyl acetate) (EVA) copolymers with different VA contents were investigated with high-resolution nuclear magnetic resonance spectroscopy (NMR). It was found that most of the VA segments are isolated in the main chain, though three kinds of sequence distributions (VA–VA head to tail, VA–E–VA head to tail, and VA–E–E–VA head to tail) exist in the EVA copolymers with higher VA content. Furthermore, two kinds of alkyl-branching signals were detected in the high temperature <sup>13</sup>C NMR spectra of EVA copolymers. Solid-state <sup>13</sup>C NMR spectroscopic investigation indicated that only orthorhombic phase exists in the crystalline region of the EVA copolymers with lower VA content. For the EVA copolymers with higher VA content, however, besides the occurrence of orthorhombic crystalline phase, monoclinic phase was also detected. As a metastable state, monoclinic phase is mainly affected by VA content as well as the thermal treating history.

© 2004 Elsevier Ltd. All rights reserved.

**Keywords:** EVA copolymers; Sequence distribution; Polymorphism

## 1. Introduction

In the last several decades, due to their unique chain structure and crystalline behavior, semi-crystalline copolymers have been widely investigated [1–4]. A common conclusion was obtained that the chain structure of polymers has important effect on the phase structures and the ultimate physical and mechanical properties of polymeric materials. Meanwhile, without an essential understanding of the condensed state structure, it is impossible to obtain adequate, predictive structure–property correlations [5]. High-resolution NMR, either solution or solid-state spectra, can provide abundant structure information and has been paid more attention in recent years, capable of elucidating not only the details of the chemical structure of a polymer,

but also its dynamic behavior. More importantly, solid state NMR spectroscopy provides an effective tool for probing the condensed state structure of polymers [6–13].

As a representative semi-crystalline random copolymer, EVA is of great industrial importance. It is a typical amphoteric polymer composed of hydrophobic and hydrophilic segments and its property is expected to vary widely with the copolymer composition, for example, the copolymers become completely amorphous when the VA content exceeds 50 wt%. As EVA is produced by low pressure, free radical polymerization process, it also exhibits an alkyl-branching pattern, similar to that of LLDPE. With the help of high-resolution NMR techniques, the sequence distribution and condensed state of EVA copolymers can be clearly characterized, helping to further understand the structure–property correlations of the corresponding materials on a molecular level.

Understanding the mechanism of the polymorphism

\* Corresponding authors. Tel.: +86-1082618533; fax: +86-1062569564.  
E-mail addresses: [djwang@iccas.ac.cn](mailto:djwang@iccas.ac.cn) (D. Wang), [xudf@iccas.ac.cn](mailto:xudf@iccas.ac.cn) (D. Xu).

formation and its influencing factors is another very important subject for elucidating the crystallization behavior of ethylene copolymers. It is known that polymorphism is a common phenomenon for orientated ethylene copolymers, which has been investigated for many years, and several viewpoints have been put forward [14–16]. However, the mechanism of the polymorphism formation in EVA copolymers is still not fully understood. Systematic investigations on the morphology and crystalline behavior of PE and its co-polymers with acrylic acid or  $\alpha$ -octene have been carried out in our laboratory [17–21]. With the help of high-resolution cryogenic FTIR spectroscopy, we have previously proven that polymorphism can and does exist in unorientated ethylene copolymers with long side group and higher side group content. The purpose of this study is to investigate the sequence distribution and crystallization behavior of a series of EVA copolymers with the help of high-resolution NMR technique, in order to get more comprehensive understanding of the correlations between chain structure and condensed state structure of ethylene copolymers.

## 2. Experimental section

### 2.1. Materials and sample preparation

EVA samples were obtained from Beijing Organic Chemical Factory and their physical parameters were listed in Table 1.

In this work, the sample used for solid-state NMR measurements was a thin film that can be cut, rolled and packed into a rotor with relative ease. The sample films were obtained by melt-pressing process, and the melting temperature was 40 °C higher than the melting point of the samples. To investigate the influence of thermal history on the crystallization behavior, two methods were used to prepare the target thin films: (1) air cooling method, the films were obtained by switching off the heater to let the molten films cool down slowly; (2) quenching method, the films were obtained by immersing the molten films in

liquid nitrogen so that the temperature of the samples decreased rapidly.

### 2.2. Measurements

#### 2.2.1. NMR

All NMR spectra were recorded on a Bruker-AM 300 NMR spectrometer, operated at 300.13 and 75.47 MHz for  $^1\text{H}$  NMR and  $^{13}\text{C}$  NMR, respectively. The solution NMR measurements were performed at a high probe temperature (100 °C) using a 90° pulse angle. The samples were mostly run either as 5% ( $^1\text{H}$ ) or 20% in ( $^{13}\text{C}$ ) solutions in deuterated *o*-dichlorobenzene. In the process of studying the phase structure of EVA copolymers with high-resolution solid  $^{13}\text{C}$  NMR, cross-polarization and magic-angle spinning (CP-MAS) and single pulse excitation/magic-angle spinning (SPE/MAS) techniques were adopted. The CP parameters used were as follows: 90° pulse with 2  $\mu\text{s}$  width, 1 ms contact time and 3 s recycle time, 4 mm rotors rotating at 4 kHz, and scan number 2400. The SPE parameters used were as follows: 90° pulse (4 s delay), high power proton decoupling.

#### 2.2.2. FTIR

FTIR spectra of all samples were recorded on a Nicolet Magna 750 FTIR spectrometer with 1  $\text{cm}^{-1}$  resolution and 64 scans. A MCT detector was used to acquire higher-resolution IR spectra. To improve the spectral resolution, a cryogenic technique was applied, and the temperature of the samples was controlled at ca. –195 °C in the process of spectra collection [22].

#### 2.2.3. DSC

The melting point  $T_m$  and crystallization point  $T_c$  of each EVA sample were measured using a Mettler DSC 822e differential scanning calorimeter at a heating rate of 10 K/min, and the sample weight was ca. 10 mg. Indium was used as the standard sample.

## 3. Results and discussion

### 3.1. Sequence distribution of EVA copolymers

NMR spectroscopy is a powerful tool for the analysis of the molecular chain structure of polymers. Fig. 1 shows the high-temperature solution  $^{13}\text{C}$  NMR spectra of a series of EVA copolymers with different VA content. Each  $^{13}\text{C}$  NMR spectrum is composed of several peaks, and from which we can classify every carbon atom in the EVA molecular chain, based on the chemical shift of each peak. The results were listed in Table 2.

According to the difference of the chemical shift of each carbon atom, the molecular chain structure of EVA

Table 1  
Basic properties of EVA copolymers

| Sample code | Co-monomer |      | $d$ ( $\text{g}/\text{cm}^3$ ) | $T_m$ (°C) | $T_c$ (°C) | MI<br>( $\text{g}/10$ min) |
|-------------|------------|------|--------------------------------|------------|------------|----------------------------|
|             | wt%        | mol% |                                |            |            |                            |
| EVA (9)     | 9          | 3.3  | 0.932                          | 98         | 88         | 2                          |
| EVA (14)    | 14         | 5.0  | 0.935                          | 88         | 72         | 2                          |
| EVA (18)    | 18         | 6.7  | 0.940                          | 84         | 69         | 3                          |
| EVA (28)    | 28         | 11.2 | 0.955                          | 65         | 52         | 150                        |
| EVA (40)    | 40         | 17.8 | 0.980                          | 49         | 30         | 50                         |

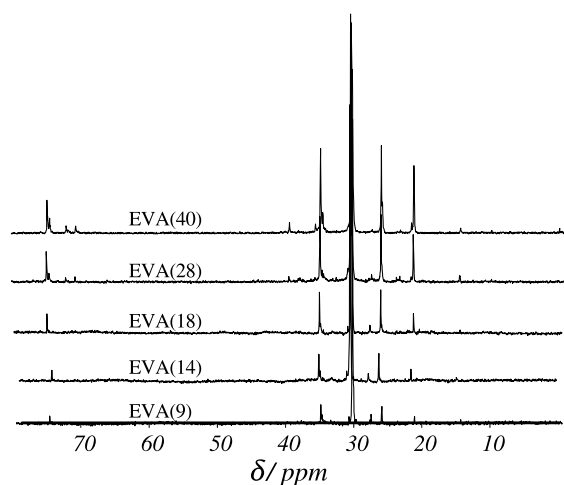
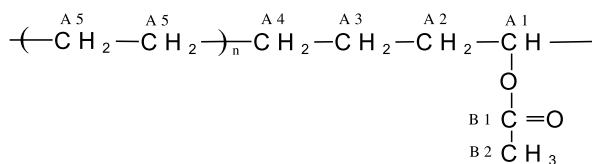


Fig. 1. High temperature <sup>13</sup>C NMR spectra of EVA copolymers.

copolymers can be labeled as below:



Due to the interaction among neighboring side groups, the chemical shifts of carbon atoms in the main chain will change with the variation of VA content. Because the VA content is very small in EVA (9) (ca. 3.3 mol%), the interactions among the acetate groups can be neglected, consequently each side acetate group is considered as isolated moiety. Therefore, making use of the chemical shifts of EVA (9) and the chemical shift of ethylene segment (30 ppm), a set of correction parameters ( $\delta_c$ ) to the chemical shifts of <sup>13</sup>C can be obtained (Table 3) [23]. In Table 3, C $\gamma$  is the farthest carbon atom which is affected by the acetate group, so a preliminary conclusion can be drawn that each VA segment can be considered as an isolated structure if the total number of carbon atoms between neighboring methine carbon atoms is equal to or more than six. If this number is less than six, the chemical shift of each carbon atom in the sequence can be obtained with the help of  $\delta_c$  (Table 4). In

Table 2 <sup>13</sup>C chemical shifts (ppm) of EVA copolymers in <sup>13</sup>C NMR spectra

| Carbon atom | EVA (40) | EVA (28) | EVA (18) | EVA (14) | EVA (9) |
|-------------|----------|----------|----------|----------|---------|
| A1          | 73.96    | 73.96    | 74.40    | 74.38    | 74.42   |
| A2          | 34.43    | 34.43    | 34.63    | 34.63    | 34.63   |
| A3          | 25.64    | 25.62    | 25.69    | 25.69    | 25.70   |
| A4          | 30.48    | 30.47    | 30.49    | 30.47    | 30.49   |
| A5          | 30.00    | 30.00    | 30.00    | 30.00    | 30.00   |
| B1          | 169.80   | 169.78   | 169.93   | 169.85   | 169.82  |
| B2          | 20.90    | 20.95    | 20.90    | 20.90    | 20.93   |

Table 3 Correction parameters of VA side branch to the chemical shifts of <sup>13</sup>C NMR spectra

|               | $\delta_c$              |
|---------------|-------------------------|
| $-\text{CH}-$ | $74.42 - 30.00 = 44.42$ |
| C $\alpha$    | $34.63 - 30.00 = 4.63$  |
| C $\beta$     | $25.70 - 30.00 = -4.30$ |
| C $\gamma$    | $30.49 - 30.00 = 0.49$  |
| C $\delta$    | 0.00                    |

Table 4, the carbon atoms enclosed by the dotted lines correspond to those contained in isolated VA sequence. Whether the six kinds of sequence structures listed in Table 4 exist in EVA copolymers or not depend on the chemical shifts which are outside of the region enclosed by two dotted lines. In another word, if the chemical shifts which are outside of the said region were detected in the solution <sup>13</sup>C NMR spectrum, we can say that this kind of sequence structure exists in EVA copolymer.

By comparing the data in Table 4 with those obtained from Fig. 1, only chemical shifts enclosed inside the dotted region can be found from the solution <sup>13</sup>C NMR spectra of EVA (9) and EVA (14), so we can deduce that the total carbon atom number between neighboring methine carbon atoms is more than six and all the side acetate groups are isolated. For the solution <sup>13</sup>C NMR spectrum of EVA (18), however, besides the chemical shifts which were surrounded by the dotted lines, the chemical shifts 21.40, 35.12, and 30.98 ppm were also detected, meaning that sequence structures 2 and 4 listed in Table 4 exist in the molecular chains of EVA (18) copolymer. Similarly, the chemical shifts of 39.26, 70.12, 35.12, 21.40, 35.12, and 30.98 ppm were detected in EVA (28) and EVA (40) copolymers, indicating that three kinds of sequence structures (2, 4, 6) exist in EVA (28) and EVA (40) copolymers. Among the different sequence structures, 2 corresponds to the VA–VA head-to-tail structure, 4 the VA–E–VA head-to-tail structure, 6 the VA–E–E–VA head-to-tail structure. By comparing the signal intensities of isolated and unisolated sequence structures, we can get a conclusion that most of the VA sequences are isolated in EVA copolymers.

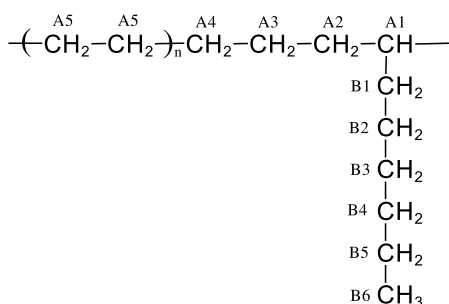
As EVA copolymers were produced by a low-pressure, free radical polymerization process, they may have alkyl-branching patterns, similar to that of LLDPE. We can see the signals of the alkyl branches from high temperature solution <sup>13</sup>C NMR spectra. Randall has studied all kinds of side chain’s chemical shifts possibly existing in LLDPE [24], which can be taken as the reference for ascertaining the types of alkyl branches existing in EVA copolymers. The results in Table 5 indicate that there are two kinds of alkyl branches in EVA copolymers, the length of which decreases with increasing ethylene segments content. Corresponding

Table 4

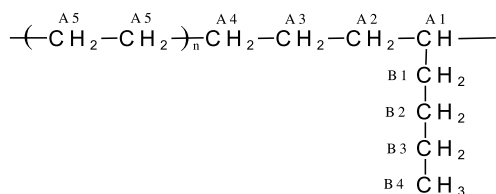
Calculated chemical shifts (ppm) of different positioned carbon atoms in several sequence structures for EVA copolymers

|   | C1    | C2    | C3    | C4    | C5    | C6    | C7    |
|---|-------|-------|-------|-------|-------|-------|-------|
| 1 | 79.05 | 30.33 | 26.19 | 30.49 | 30.00 |       |       |
| 2 | 39.26 | 70.12 | 35.12 | 34.63 | 30.49 | 30.00 |       |
| 3 | 30.33 | 74.91 | 34.63 | 25.70 | 30.49 | 30.00 |       |
| 4 | 21.40 | 35.12 | 74.42 | 34.63 | 25.70 | 30.49 |       |
| 5 | 26.19 | 34.63 | 74.42 | 34.63 | 25.70 | 30.49 |       |
| 6 | 30.98 | 25.70 | 34.63 | 74.42 | 34.63 | 25.70 | 30.49 |

molecular chains were described as below:



*n*-hexyl branch: EVA (28), EVA (40).



*n*-butyl branch: EVA (9), EVA (14), EVA (18).

### 3.2. Crystallization behavior of EVA copolymers

Investigation of the crystallization behavior of EVA copolymers with high-resolution solid NMR has been subjected to extensive studies in the past years [25–27]. The signals of methylene peaks between 20 and 40 ppm are commonly used to describe the crystallization behavior of ethylene copolymers. As polyethylene (PE) often consists of crystalline region and non-crystalline region, the <sup>13</sup>C NMR

spectra of EVA copolymers can also be well resolved into the crystalline and amorphous contributions, because the crystalline phase of ethylene copolymers is mainly composed of ethylene segments.

Fig. 2 shows the <sup>13</sup>C SPE/MAS and CP/MAS NMR spectra of EVA (9) thin film prepared with air-cooling method. The assignments of the NMR chemical shifts are expressed as following: the peak at 75 ppm corresponds to the methine carbon atoms that directly connect with VA side groups. The peak positions of C<sub>α,≥δ</sub> and C<sub>β,≥δ</sub>, which are close to the methine carbon atoms, are located at 35 and 27 ppm, respectively. The peaks at 30 and 32 ppm are assigned to the amorphous state and orthorhombic packing of ethylene segments, respectively. Generally, the pulse sequence of CP/MAS can depress the signals of non-crystalline region and enhance the signals of crystalline region correspondingly, while the pulse sequence of SPE/MAS favors the signals of non-crystalline region of semi-crystalline polymers. It was observed from Fig. 2 that the signal of orthorhombic crystal (32 ppm) decreases obviously in the SPE/MAS NMR spectrum, while the signal of amorphous region (30 ppm), the signals of C<sub>α,≥δ</sub> and C<sub>β,≥δ</sub>, and the signal of the methine carbon atoms are enhanced distinctly. Similar trends were obtained for the other EVA copolymers. These results indicate that not only VA side groups and the methine carbon atoms but also α and β carbon atoms in the ethylene segments do not enter the crystalline lattice.

Fig. 3 shows the <sup>13</sup>C CP/MAS NMR spectra of quenched EVA copolymers. The signals of crystalline region of EVA copolymers decrease with VA content increasing, indicating that the crystallinity decreases with the increase of VA

Table 5  
Chemical shifts (ppm) of branch structures in EVA copolymers

|                     | A1   | A2   | A3   | A4   | A5   | B1   | B2   | B3   | B4   | B5   | B6   |                        |
|---------------------|------|------|------|------|------|------|------|------|------|------|------|------------------------|
| Randall's data      | 38.2 | 34.6 | 27.4 | 30.5 | 30.0 | 34.7 | 27.4 | 30.0 | 32.3 | 22.9 | 14.1 | <i>n</i> -Hexylbranch  |
| EVA (28)            | 38.4 | 34.6 | 27.3 | 30.5 | 30.0 | 34.6 | 27.3 | 30.0 | 32.3 | 22.8 | 14.1 |                        |
| EVA (40)            | 38.4 | 34.7 | 27.3 | 30.5 | 30.0 | 34.7 | 27.4 | 30.0 | 32.3 | 22.8 | 14.0 |                        |
| Randall's data [24] | 38.2 | 34.6 | 27.2 | 30.6 | 30.0 | 34.3 | 27.3 | 23.3 | 14.0 |      |      | <i>n</i> -Butyl branch |
| EVA (9)             | 38.3 | 34.6 | 27.4 | 30.5 | 30.0 | 34.4 | 27.4 | 23.3 | 14.1 |      |      |                        |
| EVA (14)            | 38.3 | 34.6 | 27.3 | 30.5 | 30.0 | 34.4 | 27.3 | 23.3 | 14.1 |      |      |                        |
| EVA (18)            | 38.3 | 34.6 | 27.3 | 30.5 | 30.0 | 34.4 | 27.3 | 23.3 | 14.1 |      |      |                        |

content. For EVA copolymers with higher VA content such as EVA (18), EVA (28) and EVA (40), monoclinic crystalline phase was also formed. For ethylene copolymers, monoclinic crystal is a transitional structure from spherulitic crystal to fibril structure [28,29], the formation of metastable monoclinic crystal indicates that the crystalline behavior of copolymers changes greatly with branching. The crystalline behavior and the formation mechanism of monoclinic crystal in unoriented ethylene copolymers have been seldom reported before. To obtain more detailed information about the crystalline and non-crystalline components, curve-fitting results of the NMR spectra for EVA (9) and EVOH (28) were presented as representatives in Figs. 4 and 5, respectively. Curve-fitting of NMR spectra is on the basis of  $^{13}\text{C}$  spin–spin relaxation time measurements and line shape analysis. It was observed that, the signals of the monoclinic phase are quite apparent and can be distinguished easily from the NMR spectra of EVA (28). On the contrary, the signals of the monoclinic phase in EVA (9) can hardly be observed. This result means that the copolymerization of VA group into ethylene chains leads to the formation of metastable crystalline phase, monoclinic crystal.

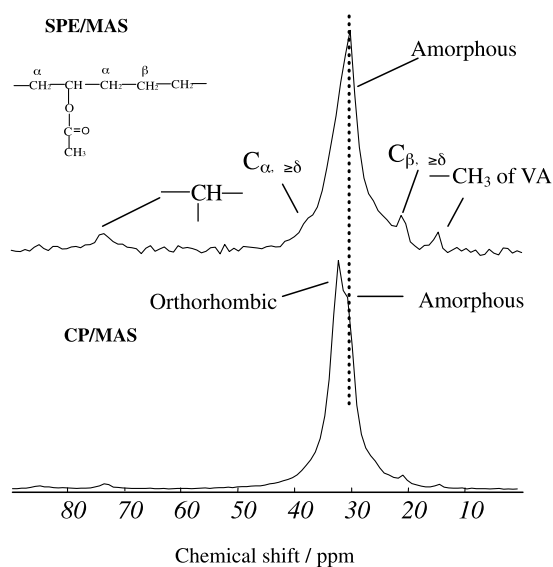


Fig. 2.  $^{13}\text{C}$  SPE/MAS and CP/MAS NMR spectra of EVA (9) prepared with air-cooling method.

Different thermal history has great influence on the crystalline states of semi-crystalline polymers. To investigate the influence of different thermal treating conditions on the crystalline behavior, two different methods were used to prepare sample films in this work: air-cooling and quenching treatment. Fig. 6 is the solid  $^{13}\text{C}$  CP/MAS NMR spectra of EVA copolymers under melting/air cooling treatment. The crystallinity and the monoclinic/orthorhombic (M/O) ratios for both quenched and air cooled samples can be calculated according to the curve-fitting results. (Fig. 7) Although the relative intensities obtained do not represent the real contents of these phase components in the samples, due to the non-quantitative nature of the CP technique, quantitative comparisons can be made of fitting results for samples with different comonomer contents. In Fig. 7, it was found that the crystallinity of air-cooled samples is larger than that of quenched ones, implying enhancing effect of the air-cooling treatment on the crystallinity of EVA copolymers. Another interesting phenomenon is that the M/O ratios of quenched samples are larger than that of air-cooling samples, meaning that quenching treatment lead to prior formation of monoclinic crystal, which will be confirmed later by the results of high-resolution cryogenic FTIR spectroscopic investigation.

It should be pointed out that, the M/O ratio does not increase linearly with branching. The M/O ratio of EVA (28) is the largest among all the EVA samples. As shown in Table 1, the  $T_m$  and  $T_c$  of EVA copolymers decrease with increasing VA content. The  $T_c$  of EVA (18) and EVA (28)

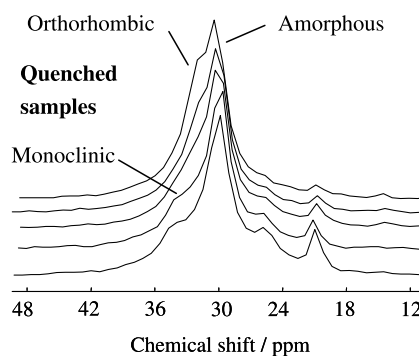


Fig. 3.  $^{13}\text{C}$  CP/MAS NMR spectra of EVA copolymers by quenching treated. From top to bottom: EVA (9), EVA (14), EVA (18), EVA (28), EVA (40).

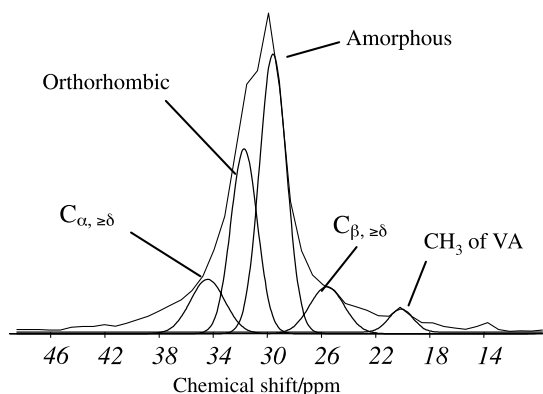


Fig. 4. Curve-fitting results of  $^{13}\text{C}$  CP/MAS NMR spectra of EVA (9) prepared with quenching method.

are 70 and 52 °C respectively, while that of EVA (40) is near 30 °C, close to room temperature. At room temperature, monoclinic crystals of EVA (40) will be partly transformed to orthorhombic crystals, leading to the relative decrease of the M/O ratio of EVA (40).

Infrared spectroscopy, as a powerful tool for the characterization of crystal lattice vibration, was used for the investigation of the crystalline behavior of EVA copolymers in this work. Four bands between 750 and 700  $\text{cm}^{-1}$  are commonly applied to describe the rocking bands of methylene group, among which 733 and 721  $\text{cm}^{-1}$  are assigned to the orthorhombic crystalline structure, 724  $\text{cm}^{-1}$  the amorphous state, and 718  $\text{cm}^{-1}$  the monoclinic crystalline structure [30–33]. To improve the spectra resolution, the temperature of the samples was controlled at ca.  $-194$  °C during the spectra collection. At low temperature, the S/N ratios of the IR spectra of EVA were significantly improved and the bandwidths decreased considerably.

Figs. 8 and 9 show the high-resolution cryogenic FTIR spectra of EVA (9) and EVA (28), respectively. The monoclinic band of EVA around 718  $\text{cm}^{-1}$ , which can hardly be seen at room temperature, appeared as a shoulder at the right side of the 721  $\text{cm}^{-1}$  peak in the cryogenic FTIR

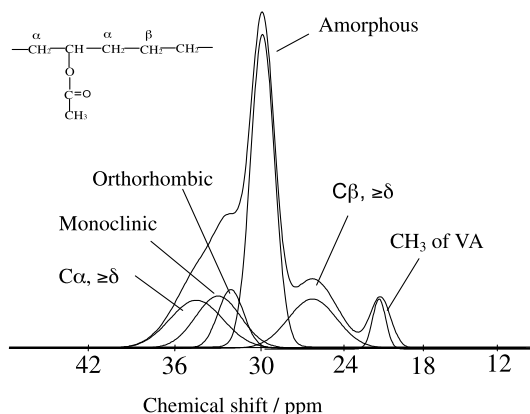


Fig. 5. Curve-fitting results of  $^{13}\text{C}$  CP/MAS NMR spectra of EVA (28) prepared with quenching method.

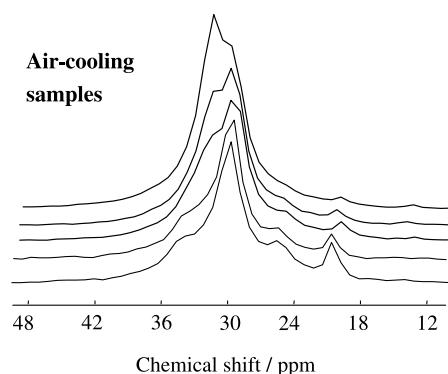


Fig. 6.  $^{13}\text{C}$  CP/MAS NMR spectra of EVA copolymers prepared with air-cooling method. From top to bottom: EVA (9), EVA (14), EVA (18), EVA (28), EVA (40).

spectra with higher VA content (EVA (28)). Its second derivative spectrum further supported the formation of monoclinic crystal. For ethylene copolymers with lower VA content (EVA (9)), only orthorhombic crystal signal (721 and 733  $\text{cm}^{-1}$ ) can be observed either from original spectrum or from second derivative spectrum. These results indicate that polymorphism can and does exist in unorientated ethylene copolymers with long side group and high side group content. FTIR results are in good agreement with the conclusion getting from the high-resolution solid NMR spectroscopic investigations.

All the above results indicated that co-monomer unit content (VA) has great influences on the crystalline behavior of EVA copolymers, not only the crystallinity but also the crystalline phase of EVA copolymers. It can be explained that the long side groups of EVA blocks the ethylene segments' movement in the crystallization process and affect the ordered packing of ethylene segments. In such a case, the monoclinic crystalline structure may become thermodynamically stable or dynamically favored. Another possible explanation is that the average sequence length of crystallized ethylene segments is shortened with the increase of acetate groups, which accordingly, induces the decrease of the crystallization ability of ethylene segments.

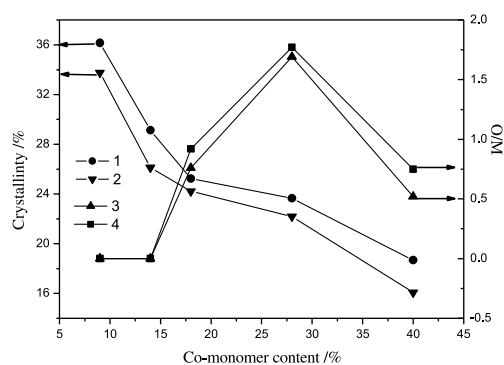


Fig. 7. Crystallinity and M/O ratio of EVA under different crystallization conditions as a function of VA content. 1. crystallinity of air cooled samples; 2. crystallinity of quenched samples; 3. M/O ratio of air-cooled samples; 4. M/O ratio of quenched samples.

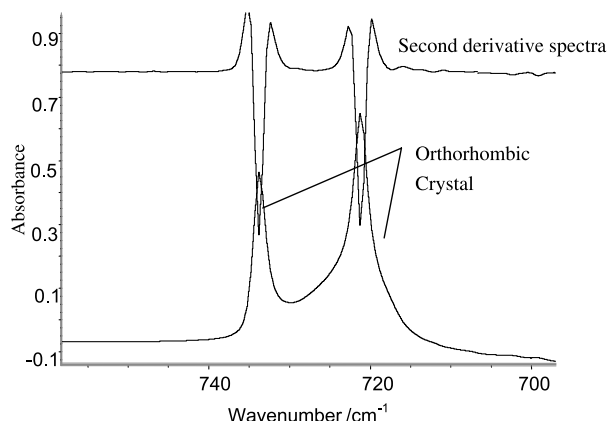


Fig. 8. High-resolution cryogenic FTIR spectrum and second derivative spectrum of EVA (9).

So, a conclusion was drawn that with the increase of VA content, the relative content of stable orthorhombic phase decreases, while that of the metastable monoclinic crystal and the amorphous phase increases. Quenching treatment made the ethylene segments frozen in ultra short time, therefore many molecular chains cannot be adjusted to the lowest energy state (orthorhombic crystal) and are confined to be thermodynamically metastable (monoclinic crystal).

#### 4. Conclusions

(1) In the molecular chain of EVA copolymers with lower VA content (EVA (9) and EVA (14)), the sequence structures are all isolated, while in EVA copolymers with higher VA content (EVA (18), EVA (28) and EVA (40)), the sequences structure are not completely isolated. In the molecular chains of EVA (18), two kinds of sequence structures (VA–VA head to tail, VA–E–VA head to tail) can be found. For EVA (28) and EVA (40), however, three kinds of sequence

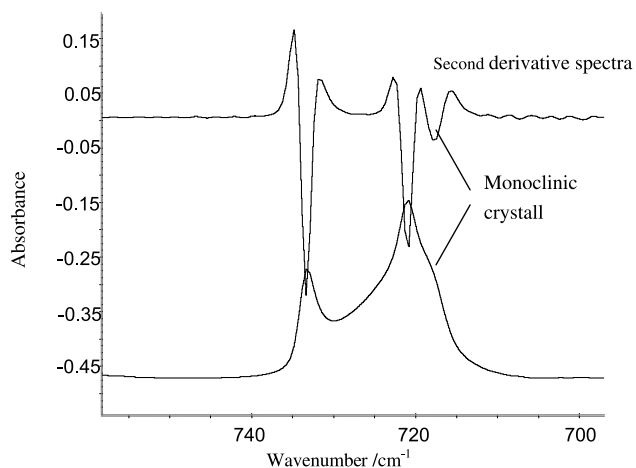


Fig. 9. High-resolution cryogenic FTIR spectrum and second derivative spectrum of EVA (28).

distributions (VA–VA head to tail, VA–E–VA head to tail, VA–E–E–VA, head to tail) exist.

- (2) Two kinds of alkyl-branching signals were detected in solution  $^{13}\text{C}$  NMR spectra of EVA copolymers. The length of alkyl-branches decreases with increasing ethylene segments content. *n*-butyl branch exists in EVA copolymers with lower VA content (EVA (9), EVA (14), EVA (18)), and *n*-hexyl branch exists in EVA copolymers with higher VA content (EVA (28), EVA (40)).
- (3) With the help of high-resolution solid NMR and high-resolution cryogenic FTIR spectroscopy, it was proved that besides the stable orthorhombic crystallite, monoclinic crystallite was also formed in the crystalline region of EVA copolymers with higher VA content. Increasing the VA content and quenching treatment are beneficial for the formation of monoclinic crystal.

#### Acknowledgements

This work was partly supported by National Natural Science Foundation of China (NSFC, Grant No. 50290090), Polymer Science and Materials Team Building Project and Directional Project from CAS.

#### References

- [1] Axelson DE. In: Komoroski, editor. High-resolution NMR spectroscopy of synthetic polymers in bulk. Weinheim: VCH Publishers; 1986. p. 157.
- [2] Klein PG, Driver MAN. *Macromolecules* 2002;35:6598.
- [3] Zhang QJ, Lin WX, Chen Q, Yang G. *Macromolecules* 2000;33:8904.
- [4] Takahashi M, Tashiro K, Amiya S. *Macromolecules* 1999;32:5860.
- [5] Bistac S, Kunemann P, Schultz J. *Polymer* 1998;39:4875.
- [6] Andrew ER. *Prog Nucl Magn Reson Spectrosc* 1971;8:1.
- [7] Hu W, Sirota EB. *Macromolecules* 2003;36:5144.
- [8] Schaefer J, Stejskal EO, Buchdahl R. *Macromolecules* 1975;8:291.
- [9] Schaefer J, Stejskal EO, Buchdahl R. *Macromolecules* 1977;10:384.
- [10] Garroway AN, Moniz WB, Resing HA. *ACS Symp Ser* 1978;No.103.
- [11] Vanderhart DL, Perez E. *Macromolecules* 1986;19:1902.
- [12] Kitamaru R, Horii F, Murayama K. *Macromolecules* 1986;19:636.
- [13] Zhang QJ, Lin WX, Yang G, Chen Q. *J Polym Sci Part B Polym Phys* 2002;40:2199.
- [14] Liu TM, Juska TD, Harrisom IR. *Polymer* 1986;27:247.
- [15] Saraf RF, Porter RS. *J Polym Sci Polym Phys Ed* 1988;26:1049.
- [16] Yan RJ, Jiang BZ. *J Polym Sci Part B Polym Phys* 1993;31:1089.
- [17] Kang N, Xu YZ, Wu JG, Feng W, Weng SF, Xu DF. *Phys Chem Chem Phys* 2000;2:3627.
- [18] Kang N, Xu YZ, Weng SF, Wu JG, Xu DF, Xu GX. The pittsburgh conference 51th anniversary, New Orleans. Book of abstract; 2000. p. 1768.
- [19] Kang N, Xu YZ, Cai YL, Xu DF, Xu JG, Xu GX. *J Mol Struct* 2001; 562:19.
- [20] Zhang HP, Xu DF, Xu YZ, Weng SF, Wu JG. *Mikrochim Acta (Suppl.)* 1997;14:425.
- [21] Zhang HP, Xu DF, Yang JY. International microsymposium on polymer physics, Xi'an. Book of abstract; 1995. p. 32.
- [22] Kang N, Xu YZ, Ferraro JR, Li WH, Weng SH, Xu DF, Wu JG, Soloway RD. *Appl Spectrosc* 2001;55:643.

- [23] Zhu SN. *Polymer chain structure*. Beijing: Science Press; 1996. p. 213.
- [24] Randall JC. *J Polym Sci Polym Phys Ed* 1973;11:275.
- [25] Kitamaru R, Horii F, Zhu Q, Bassett DC, Olley RH. *Polymer* 1994;35:1171.
- [26] Nakagawa M, Horii F, Kitamaru R. *Polymer* 1990;31:323.
- [27] Luo HJ, Chen Q, Yang G, Xu DF. *Polymer* 1998;39:943.
- [28] Peterlin A. *J Mater Sci* 1971;6:490.
- [29] Juska T, Harrison R. *Polym Engng Rev* 1982;2:14.
- [30] Hagemann H, Strauss HL, Snyder RG. *Macromolecules* 1987;30:2810.
- [31] Hagemann H, Snyder RG, Peacock AJ, Mandelkern L. *Macromolecules* 1989;22:3600.
- [32] Snyder RG. *J Chem Phys* 1979;71:3229.
- [33] Snyder RG, Maroncelli M, Strauss HL, Hallmark VM. *J Phys Chem* 1986;56:23.